EFFECT OF COKE PROPERTIES ON THE BUBBLE FORMATION AT THE ANODES DURING ALUMINIUM ELECTROLYSIS IN LABORATORY SCALE

Wojciech Gebarowski[1], Arne Petter Ratvik[1], Stein Rørvik[2], Lorentz Petter Lossius[3], Hogne Linga[3], Ann Mari Svensson[1]

[1]Dept. of Materials Science and Engineering, Norwegian University of Science and Technology, NO-7491 Trondheim, Norway

[2]SINTEF Materials and Chemistry, NO-7465 Trondheim, Norway

[3]Hydro Aluminium, Årdalstangen, Norway

Abstract The anodic reaction of aluminium electrolysis cells leads to the formation of CO_2 bubbles, which partly screen the anode surface and leads to an increase in the cell voltage. An advantage of these bubbles is that the formation and release contribute to the stirring of the electrolyte, however, the screening of the surface increase the irreversible energy losses. In this work the voltage and current oscillation due to bubbles evolution during electrolysis in laboratory cell were presented. A comparison of different carbon anode materials in terms of coke impurities (mainly sulphur content) and grain sizes were investigated. Anodes with finer coke fraction showed lower oscillations than coarser fraction equivalents. Additionally, influence of current density on amplitude of anode potentials was measured. A 64 % increase of current density caused an increase of anode potential oscillations from 79 to 179 %.

Key words: carbon anodes, aluminium electrolysis, gas bubbles

1 Introduction

The majority of primary aluminium production is based on electrochemical reduction of alumina with use of prebaked carbon anodes. During electrolysis, carbon anodes are consumed by conversion to, mainly, CO_2. Assuming a current density 0.8 $A \cdot cm^{-2}$, 0.02 M of CO_2 per 1 m^2 of anode every second is produced which gives at 960 °C a volume of about 2.13 dm^2. Due to the horizontal placement of anodes in the cells, with the active part of the electrode facing downwards, such large amount of gas produced on the surface has a significant impact on the process. According to Haupin and Kvande [1], the presence of gas bubbles in an industrial cell increases the cell voltage by 0.25 V which gives about 6 % contribution to the total cell voltage. In the literature it is very common to denote this component of the cell voltage as bubbles overpotential, which is slightly confusing, because, in fact, bubbles increase cell voltage by two main mechanisms: increase of ohmic resistance of the electrolyte and increase of activation polarization [2]. An increase of ohmic resistance of electrolyte may be described by Bruggemann's equation for dispersed bubble phase fraction in an electrolyte [3, 4]. The presence of bubbles on an anode effectively decreases active surface area, which in turn increases real current density and causes an increase of the activation polarization. Bubbles also have a beneficial influence on electrolysis, providing agitation of an electrolyte which reduces the concentration polarization.

Considering the high electrical current in an industrial cell, the presence of bubbles contributes to significant losses of energy which is a reason for considerably importance of bubbles behaviour in reduction cells. The biggest step in this matter was an implementation of slots in anodes in 1998 which substantially reduced voltage drop and voltage/current oscillations by changing of bubbles flow pattern [5]. However, still more profound understanding of bubbles formation and releasing mechanisms in order to make further improvements of process efficiency is needed.

The bubbles lifetime can be divided into two stages: nucleation and transport. Nucleation takes place on active sites which are defects and pores on the anode surface [6, 7]. Therefore, quantity nucleation sites depend on structure of anode. Subsequently, when the bubble reaches certain size, buoyancy forces detach bubble from the active site and a travel towards edge of electrode commences. The size of bubble when detaching occurs is influenced by wetting angle between electrolyte and anode. The better wetting of anode by electrolyte the smaller bubbles are detached [8, 9]. Transport stage is controlled by anode shape, inclination, surface roughness, electrolyte flow and wetting properties. Additional phenomenon that occurs in both stages is coalescence of bubbles. Bubbles may coalesce at nucleation site when two adjacent bubbles overlap during growth. Coalescence can also happen during bubbles movement when two bubbles collide.

Previous studies of bubbles in aluminium electrolysis process can be separated into three groups: i) measurements in industrial environment ii) measurements in lab scale and iii) theoretical physical models. The first group has provided very direct and practical results, but has some limitation in the control of parameters in the complex process, which is more convenient in the case of laboratory experiments. In most of laboratory studies, graphite is used as an anode material for investigations and only few papers focus on the influence of carbon materials on bubbles evolution during electrolysis. A significant discrepancy in bubbles behaviour between graphite and carbon anodes has been found in a study using various anodes of different, single source cokes [10]. The study was however limited to coke material of a low fraction, 0-2 mm, which is significantly lower than the industrial standard.

Aim of this work is to investigate correlation between carbon anodes properties and formation of bubbles in laboratory cell, including the development of bubble oscillation patterns over time, and at various operating current densities. Sample anode materials were different in terms of impurities level, mainly sulphur, as well as size of coke grains used, 0.2 mm and 0-6 mm.

Materials and Methods

The experiments were conducted in the cell depicted in Figure 1. The cell was made of graphite crucible (G330, Tokai Carbon) and placed in closed cylindrical metal reactor which in turn was placed in the resistance furnace with controlled temperature. During experiments, inert atmosphere inside reactor was maintained by passing argon at flow of 200 $ml \cdot min^{-1}$.

Table 1 Properties of cokes and anodes used for measurements

	coke 1		**coke 2**		**coke 3**	
impurities						
S /wt%	1.42		5.54		3.56	
V /ppm	116		432		402	
Ni /ppm	192		192		210	
Fe /ppm	178		316		264	
anode properties						
coke fraction	<2 mm	<6 mm	<2 mm	<6 mm	<2 mm	<6 mm
density /$g \cdot cm^{-2}$	1.56	1.65	1.63	1.62	1.64	1.63
permeability /nPm	3.53	0.44	0.57	1.39	0.30	0.44

As an electrolyte alumina saturated cryolite melt was used with following composition: 76.15 wt% of Na_3AlF_6 (≥ 97 %, Sigma-Aldrich), 11 wt% of AlF_3 (in-house sublimed from industrial grade), 4.5 wt% of CaF_2 (≥ 99.8 %, Merck), 8.35 wt% of Al_2O_3 (≥ 99.5 %, Merck) with acidity of melt CR = 2.2. During experiment alumina parts immersed in a melt dissolves preventing depletion from saturated state. Temperature of electrolyte was maintained at 960 °C providing a superheat of about 26 °C. The cylindrical crucible acted as a cathode and its sidewall was shielded by sintered alumina cover so that only bottom was as a working part. In case of non-saturated melt silicon nitride cover was used instead. Anodes had cylindrical shape and were made of anode carbon materials (Fig. **2**). Electrodes were shielded by sintered alumina to ensure that exposed surface area of the electrode was mainly horizontal. As a current lead a stainless steel tube connected with the carbon anode by threaded end was used. Inside the current lead a sense wire was placed, insulated from the main lead by alumina tube. The sense wire was connected close to the working electrode to avoid significant voltage drop across the current lead.

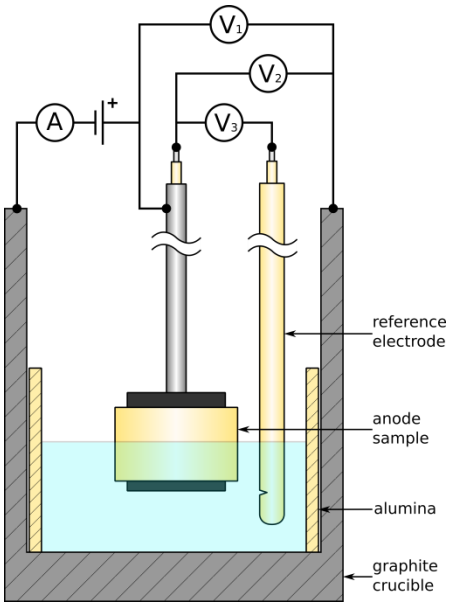

Fig. 1 Experimental setup of electrochemical cell with simplified scheme of electrical connections. V1 – cell voltage; V2 – working electrode (sense point) vs. counter electrode (crucible); V3 – working electrode (sense point) vs. reference electrode. (thermocouple and auxiliary electrode are not shown for clarity of drawing)

The anodes were made of three different one source calcined petroleum cokes which varied in content of impurities and isotropy. Each coke was used to manufacture two anode materials with coke grains fractions up to 2 and 6 mm. The pitch level was identical for both fractions and between cokes varied less than 0.4 wt%, having average value of 14.42 wt% with respect to green paste. The properties of cokes and anodes prepared from them are summarized in **Table 1**.

Potentials of working electrodes were measured against aluminium reference electrode made by placing pure aluminium in sintered alumina tube (boron nitride in case of non-saturated electrolyte) with hole to let electrolyte into tube providing ionic contact. Tungsten wire was used as an electrical contact to the aluminium pool.

As a power source a laboratory power supply unit (Agilent 6032A) controlled by LabVIEW software was used. Sense inputs of the power supply were connected to the same points as V1 (see **Fig. 1**). Three voltages and current (with use of 50 mΩ shunt resistor) were logged simultaneously using ADC module (National Instruments NI 9225) with speed 100 Sa/s. Input impedance of the module is high enough to not load the reference electrode.

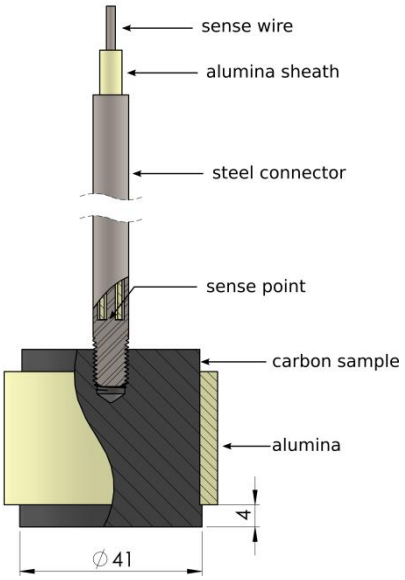

Fig. 2 Electrode assembly used for bubbles oscillations measurements.

Results and Discussion

The procedure for each sample consisted of electrolysis at constant current (CC) density 1 $A \cdot cm^{-2}$ as well as at constant voltage (CV) with keeping average current density 1 $A \cdot cm^{-2}$. This allowed observing potential and current oscillation due to bubbles releasing during CC and CV period respectively. Voltage for CV mode was determined based on the average value of last 15 seconds of voltage oscillations from the preceding CC mode. Figure 3 shows voltages recorded at three different points corresponding to V1, V2 and V3 in Figure 1 during CV mode. Discrepancies in regulation of different points are clearly visible.

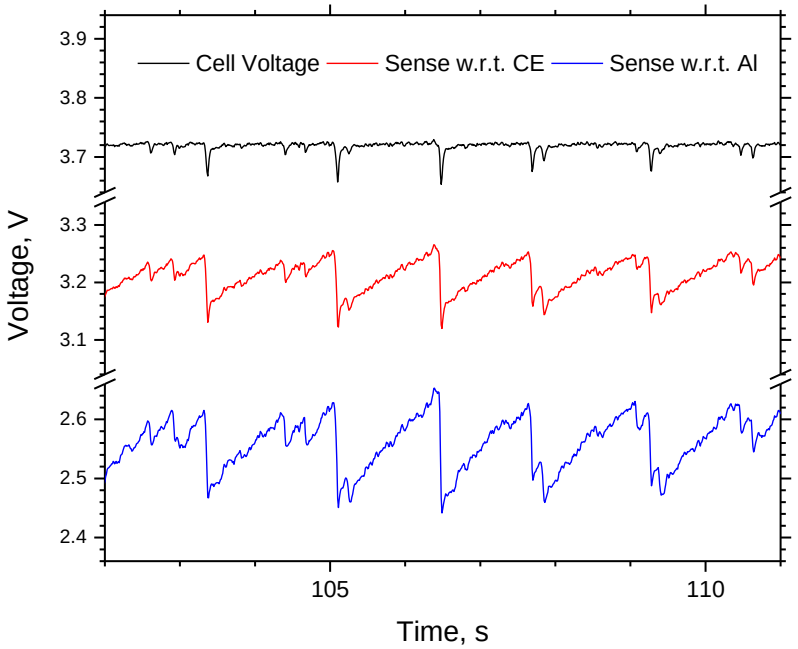

Fig. 3 Voltage measured at different points during constant voltage electrolysis.

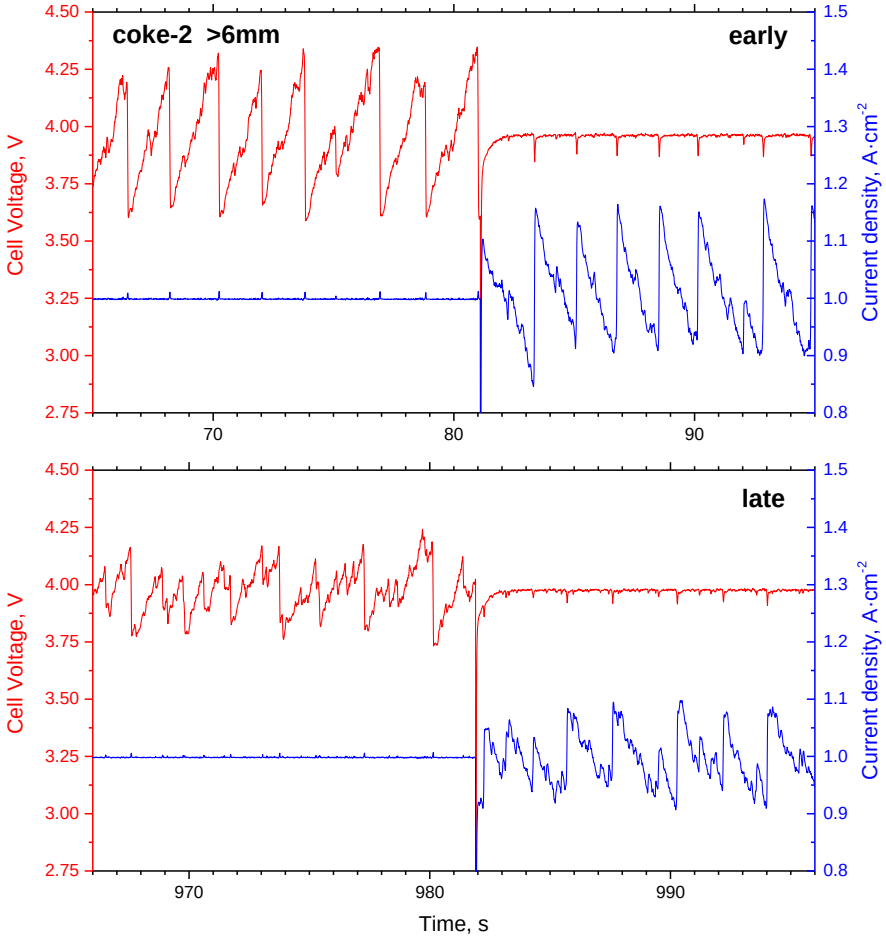

Fig. 4 Switch from oscillations of cell voltage at constant current (CC) mode to oscillations of current at constant voltage (CV) mode electrolysis. The top graph is recorded between 60 and 100 s, and the bottom graph between 960 and 1000 s.

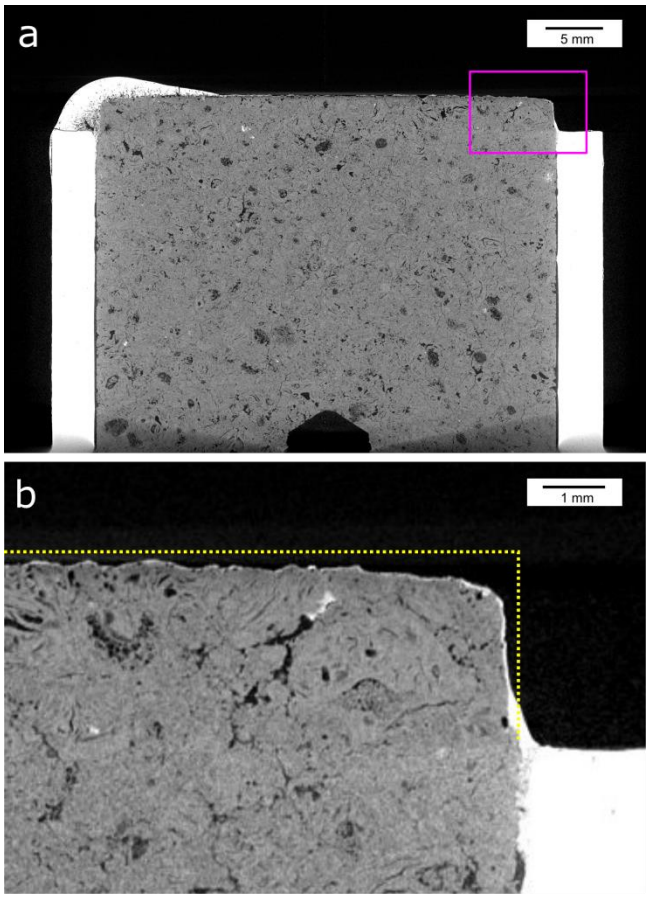

Fig. 5 Compute tomography of carbon sample after experiment. a) whole electrode; b) zoomed edge. Dotted line presents the outline of electrode before polarization.

Considering the relatively high currents and rapid changes of load due to bubbles oscillations, even moderately low inductances of anode and cathode leads caused voltage oscillations – the greater the further from the sense points of power supply (sense inputs of the power supply were connected across the cell voltage – V1 – therefore this voltage is the best regulated in CV mode).

Error! Reference source not found. shows cell voltage oscillations in the CC mode with switch to the CV mode where, in contrast, oscillations of current are visible. The shapes of voltage and current oscillations are qualitatively similar, except for the fact that one is inverted with respect to another. The oscillations obviously reflects changes in active surface area of anode due to growth of gas bubbles and their release after reaching certain size of bubble. The growth of bubbles decreases the active surface area causing an increase of real current density in the

CC mode, which causes an increase of the anode potential until a bubble is released, and then a rapid drop of voltage is observed.

Correspondingly, in CV mode, a decrease of active surface area causes a decline of current because the voltage is fixed, and the release of bubbles produce a rapid increase of current. The two graphs in **Error! Reference source not found.** represent early and late stage of electrolysis. During the early stage (first minutes), the oscillations are very regular with saw tooth shaped waveform. The amplitudes are ~ 0.75 V and ~ 0.3 $A \cdot cm^{-2}$ in CC and CV mode respectively. In the later stage of electrolysis, the oscillations are much less regular and have smaller amplitudes – ~ 0.5 V and ~ 0.2 $A \cdot cm^{-2}$, respectively. The changes in the oscillations illustrate the change of the bubbles release pattern with time. At the beginning, a machined anode has smooth surface and sharp edge. Smooth surface facilitates the growth of larger bubbles. Additionally, a sharp edge is a barrier which prevents bubbles escape from a horizontal part of an anode. Therefore, bubbles can grow larger screening a bigger surface of anode before they leave the surface. Flow patterns seems to be well ordered.

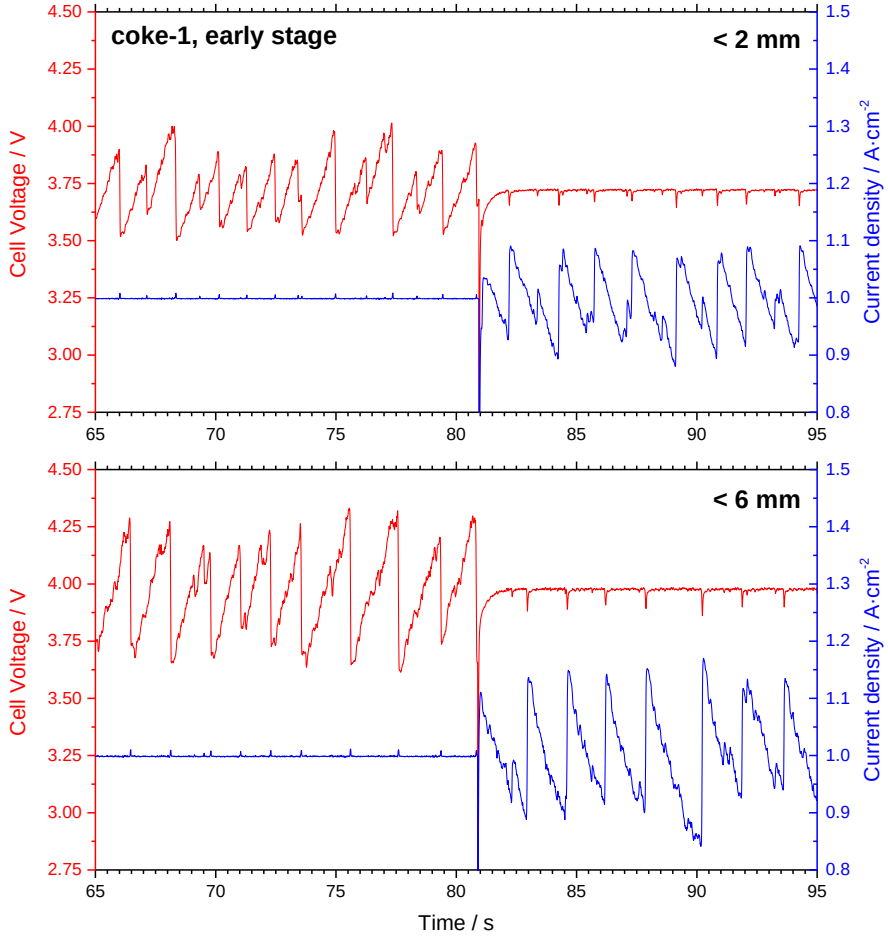

Fig. 6 Comparison of voltage and current oscillations in early period for coke 1 with fraction <2 mm (top figure) <6 mm (bottom figure).

With time of electrolysis the surface of an anode becomes rougher due to preferential oxidation of binder phase of carbon matrix. What is more, because of higher local current density on the edges of anode, a consumption of this area is higher causing rounding of the electrode edges. These two effects are depicted in **Error! Reference source not found.** where the surface of an anode after experiment is shown. Therefore, rougher surface enables more paths for bubbles movements across anode surface and rounded edges improve the ease of releasing of smaller bubbles, hence the flow pattern is more random what is clearly visible in the shape of the oscillations.

Error! Reference source not found. shows the oscillations of cell voltage and current density during an early period of electrolysis for the same anode material, but different coke fractions. In case of <2 mm coke fraction smaller amplitude of voltage and current oscillations in respect to <6 mm fraction is observed. It means that in the latter case bigger bubbles were released. Smaller bubbles in case of smaller coke fraction results from the presence of larger number of active sites where bubbles can nucleate.

The graph in **Error! Reference source not found.** contains a comparison of anode potential oscillations in CC mode for all three materials, each in two variations of coke grain sizes. Instead of amplitude of oscillation a standard deviation of mean the value of the potential was chosen. This provides a more representative statistic description of the oscillations, avoiding effects of single events (single big spikes). For all samples, a decrease of oscillations with time was observed during electrolysis, which may be attributed to changes of electrode shape and roughness. The highest oscillations for <2 mm fraction was measured for coke 1 in both early and late stage of electrolysis. The coke 1 has the lowest content of sulphur. In case of <6 mm fraction, coke 2 shows the highest oscillation amplitudes in early and late stage. The coke 2 has the highest content of sulphur. This extreme divergence can be explained when looking at permeability values for anodes – both materials (coke 1 <2 mm and coke 2 <6 mm) have the highest permeability. By comparing only anodes with a low permeability (coke 1, 0-6 mm, coke 2, 0-2 mm and coke 3, both fractions), we observe that the voltage oscillations are similar, and lowest for coke 2, with the highest sulphur content. This is in line with previous results, where the most impure cokes showed the lowest voltage oscillation for anodes of 0-2 mm fraction [10]. But also in this work there were challenges with differences in permeability. Based in the results here, it is reasonable to assume that permeability affects the bubble overvoltage by the presence of surface pores, in which CO_2 bubbles are known to reside and possibly escape.

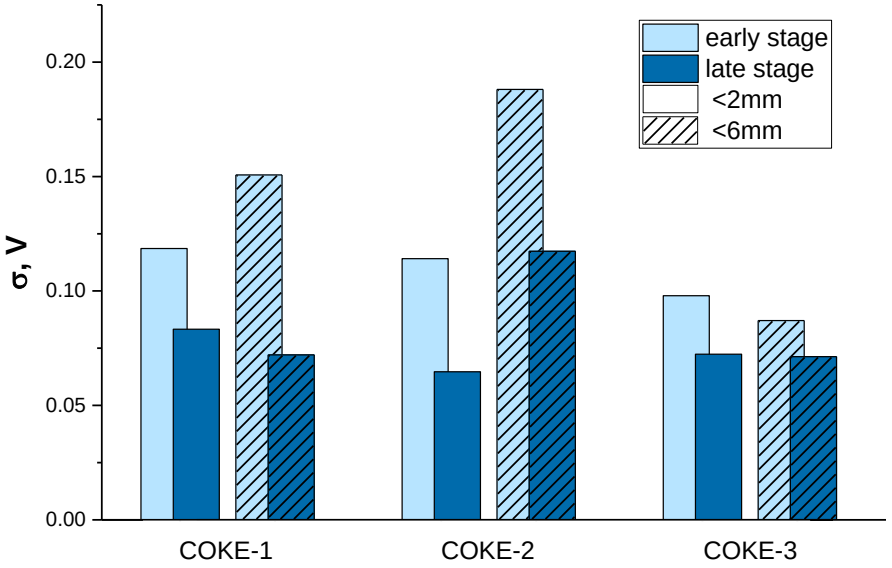

Fig. 7 Standard deviation of potentials during oscillations in CC mode at j = 1 A·cm^{-2} for different cokes in saturated electrolyte, fractions and stage of electrolysis calculated from 1 minute periods in 2-3rd and 15-16th minute of electrolysis for early and late stage respectively.

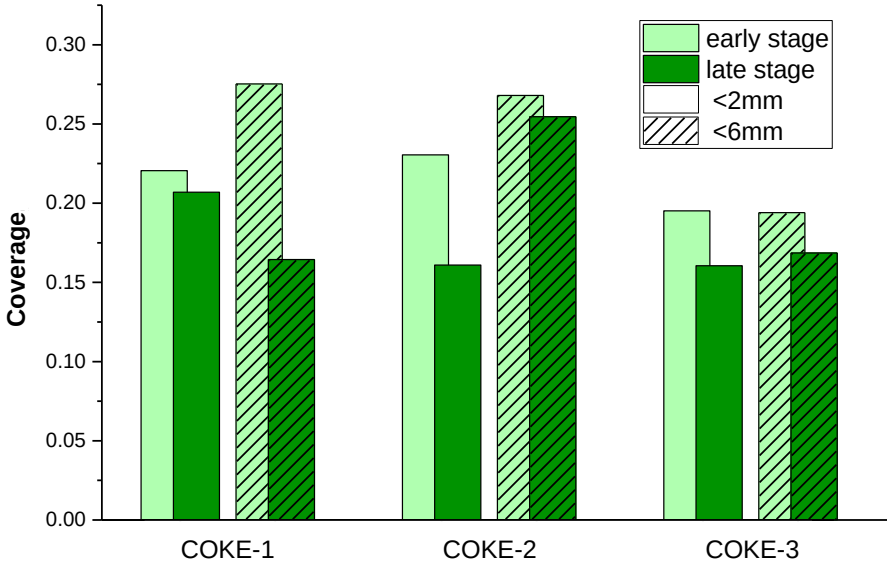

Fig. 8 Bubbles coverage of surface in CV mode at javerage = 1 A·cm^{-2} for different cokes in saturated electrolyte, fractions and stage of electrolysis calculated from 1 minute periods in 2-3rd and 15-16th minute of electrolysis for early and late stage respectively.

Oscillations of current recorded in CV mode allowed for direct calculation of a maximum fraction of an anode surface blocked by bubbles using following formula:

$$bubbles\ coverage = 1 - \frac{j_{min}}{j_{max}}$$

Results presented in **Error! Reference source not found.** are similar to the results in Figure 7, except for the highly permeable anodes, for which there are simple direct relation between potential and current oscillations.

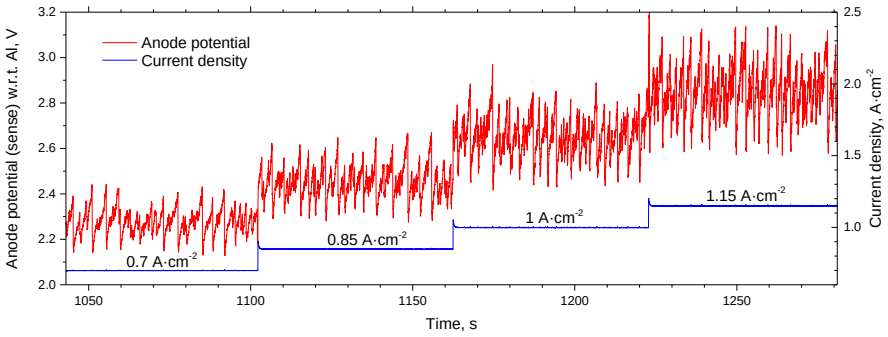

Fig. 9 Anode potential oscillations at different current densities in late period of electrolysis.

In **Error! Reference source not found.** an anode potential oscillations for increasing current densities are presented. The potentials were measured in the late stage of electrolysis. With the increase of current density, the increase of average anode potential as well as the increase of oscillation frequency and amplitudes, is visible. If one assumes a linear relation between current density and potential of an anode (activation overpotential) in range of 0.7 ÷ 1.15 A·cm^{-2}, which is reasonably correct assumption [11], a linear increase of average value of potential as well as amplitude of the oscillations with increasing current density is expected. **Error! Reference source not found.** shows the amplitudes of anode potential oscillations against current density for all anode materials. In all cases an increase of potential oscillation with increased current density is observed. The trend of these relations is relatively linear. Anodes with fraction <6 mm have higher oscillation amplitudes with respect to the <2 mm equivalents. The increase of potential oscillation amplitude between current density 0.7 and 1.15 A·cm^{-2}, is in the range 79 to 170 % which is significant value considering increase of current equal to 64 %.

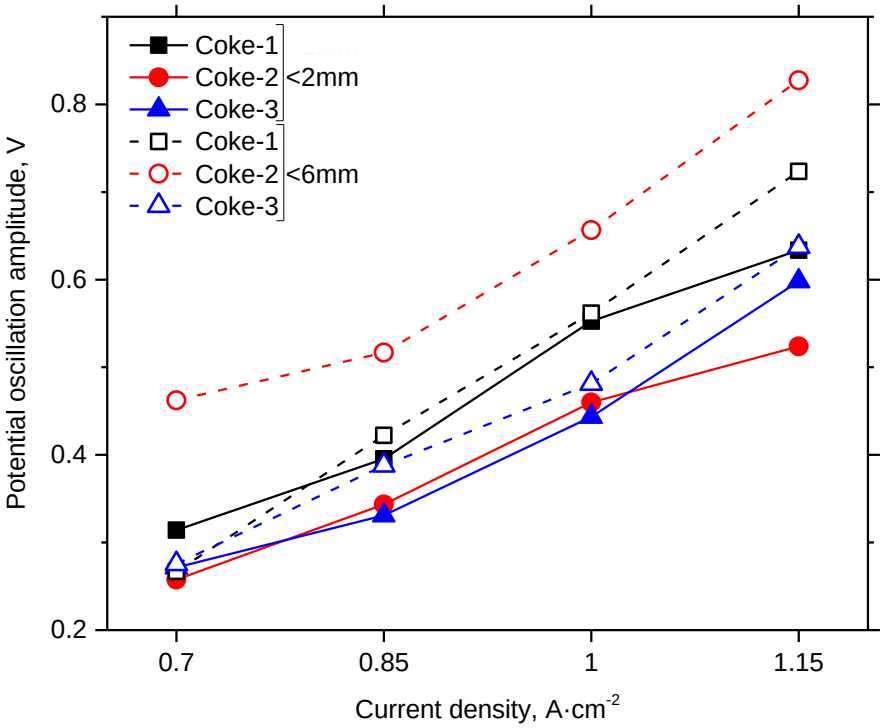

Fig. 10 Potential oscillations amplitude at different current densities for different samples.

The highest increase is observed for coke 1 <6 mm – the lowest content of sulphur. The lowest increase is observed for the coke 2 <6 mm – the highest contents of sulphur. Interestingly, this sample shows the highest amplitude of all samples for all current densities. However, as mentioned before, it can be related to the high permeability of this material.

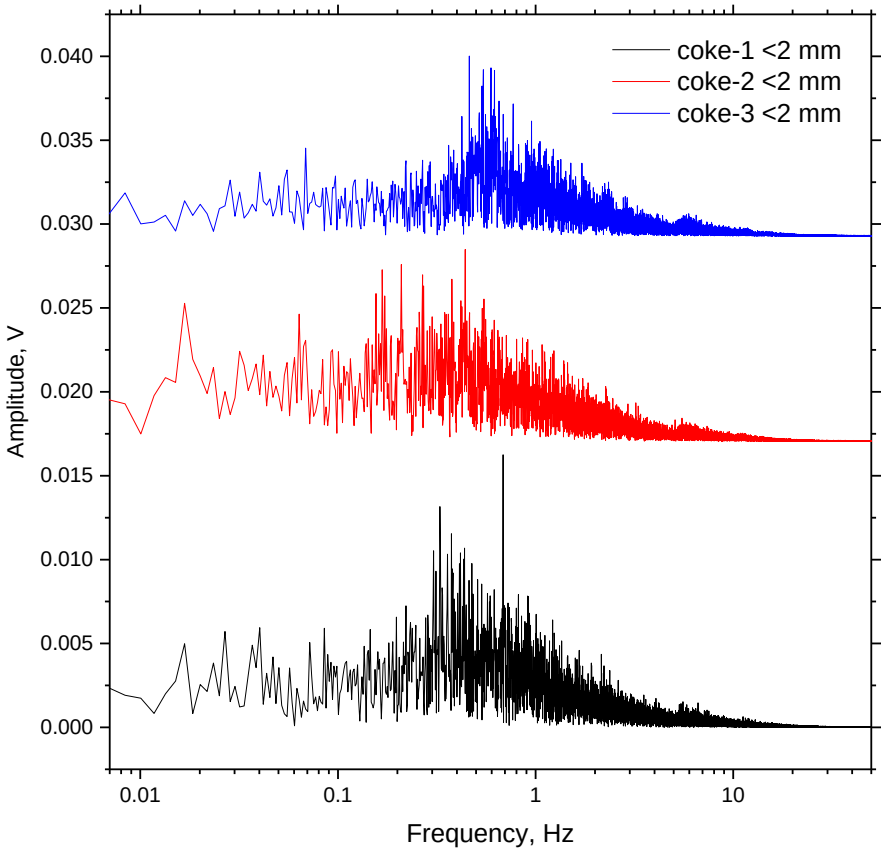

Fig. 11 FFT from the period between 8th and 16th minute of potential oscillations for <2 mm fraction anodes.

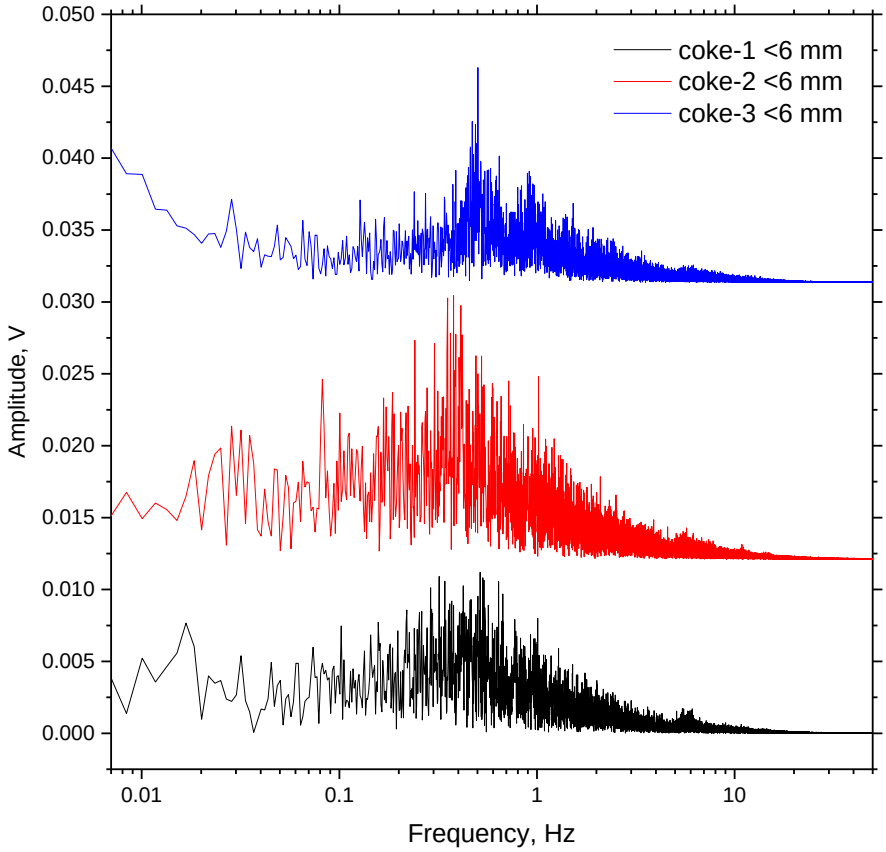

Fig. 12 FFT from the period between 8th and 16th minute of potential oscillations for <6 mm fraction anodes.

Figure 11 and 12 show FFT analysis of potential oscillations during advanced period for <2 mm and <6 mm samples respectively. The oscillations consist of components from quite wide range of frequencies with predomination of lower frequencies. The maximums on the spectra are around 0.3 – 0.6 Hz which corresponds to the main frequency of the oscillations. Lower frequencies are attributed to bigger bubbles releasing, whereas higher frequencies are produced by bubbles coalescences on the electrode surface as well as escaping of smaller bubbles from the electrode surface.

There are slight differences in FFT spectra. Comparing <2 mm fraction samples, for coke 3 main frequencies are shifted towards higher frequencies. Both coke 1 and coke 1 show distinguishable peaks whereas coke 2 has more even distribution of frequencies. In case of <6 mm fractions, coke 3 shows the sharpest peak at main frequency, while coke 1 and coke 2 have more low frequency components. Thus, the <6 mm fraction tend to produce larger bubbles.

Conclusions

In this work voltage and current oscillations caused by bubbles during electrolysis of different coke materials were studied. Presented results can be summarized in following points:

Voltage and current oscillations due to bubbles showed regular saw tooth waveform at the beginning of electrolysis and became less regular with lower amplitude with the time. These phenomena are attributed to the changes of shape and roughness of electrodes.

Anodes with coarser fraction produced higher oscillation amplitudes due to growth of larger bubbles. Finer coke fraction promotes the growth of higher number of smaller bubbles due to more active sites where nucleation of bubbles occurs.

An increase of current density from 0.7 to 1.15 $A \cdot cm^{-2}$ causes a substantial increase amplitude (from 79 up to 170 %) and frequency and of anode potential oscillations.

Correlation between coke sulphur content and bubbles behaviour is not clear and observed differences might be caused by different permeability of investigated materials. Therefore, more profound studies focused on permeability influence on bubbles oscillations are required.

Acknowledgements

This work was financed by Hydro Aluminium and the Research Council of Norway. Thanks are due to the NTNU workshop, especially to Aksel Alstad for manufacturing of experimental parts. Additionally, the contributions of Egil Skybakmoen and others at STNTEF are gratefully acknowledged.

References

1. Haupin W, Kvande H (2000) Thermodynamics of Electrochemical Reduction of Alumina. Light Met 379–384.
2. Cooksey M a., Taylor MP, Chen JJJ (2008) Resistance due to gas bubbles in aluminum reduction cells. Jom 60:51–57. doi: 10.1007/s11837-008-0019-x
3. Hine F, Murakami K (1980) Bubble effects on the solution IR drop in a vertical electrolyzer underfree and forced convection. J Electrochem Soc 127:292–297. doi: 10.1149/1.2129658
4. Qian K, Chen JJJ (1997) Visual observation of bubbles at horizontal electrodes and resistance measurements on vertical electrodes. J Appl Electrochem 27:434–440. doi: 10.1023/a:1018465705058
5. Bearne G, Gadd D, Lix S, et al (2007) The Impact of Slots on Reduction Cell Individual Anode Current Variation. 305–310.
6. Einarsrud KE, Johansen ST, Eick I (2012) Anodic Bubble Behavior in Hall-Héroult Cells. Light Met 2012 875–880. doi: 10.1002/9781118359259.ch151
7. Vogt H (1997) Contribution to the interpretation of the anode effect. Electrochim Acta 42:2695–2705. doi: 10.1016/S0013-4686(97)00013-3
8. Peterson RD, Richards NE, Tabereaux AT, et al (1990) Results of 100 Hour Electrolysis Test of a Cermet Anode: Operational Results and Industry Perspective. Light Met 385–393.
9. Zhang K, Feng Y, Schwarz P, et al (2013) Computational Fluid Dynamics (CFD) Modeling of Bubble Dynamics in the Aluminum Smelting Process. Ind Eng Chem Res 52:11378–11390. doi: 10.1021/ie303464a
10. Thorne RJ, Sommerseth C, Ratvik a. P, et al (2015) Bubble Evolution and Anode Surface Properties in Aluminium Electrolysis. J Electrochem Soc 162:E104–E114. doi: 10.1149/2.0321508jes
11. Zuca S, Herdlicka C, Terzi M (1980) On porosity-overvoltage correlation for carbon anodes in cryolite-alumina melts. Electrochim Acta 25:211–216. doi: 10.1016/0013-4686(80)80045-4